Magneto-mechanical coupling effect in amorphous Co40Fe40B20 films grown on flexible substrates

Zhenhua Tang, Baomin Wang, Huali Yang, Xinyu Xu, Yiwei Liu, Dandan Sun, Lixiang Xia, Qingfeng Zhan, Bin Chen, Minghua Tang, Yichun Zhou, Junling Wang, and Run-Wei Li

Citation: Applied Physics Letters **105**, 103504 (2014); doi: 10.1063/1.4895628
View online: http://dx.doi.org/10.1063/1.4895628
View Table of Contents: http://scitation.aip.org/content/aip/journal/apl/105/10?ver=pdfcov
Published by the AIP Publishing

Magneto-mechanical coupling effect in amorphous $Co_{40}Fe_{40}B_{20}$ films grown on flexible substrates

Zhenhua Tang,[1,2,3] Baomin Wang,[2,3,a)] Huali Yang,[2,3] Xinyu Xu,[1] Yiwei Liu,[2,3] Dandan Sun,[2,3] Lixiang Xia,[2,3] Qingfeng Zhan,[2,3] Bin Chen,[2,3] Minghua Tang,[1,b)] Yichun Zhou,[1] Junling Wang,[2,3,4] and Run-Wei Li[2,3,c)]

[1]*Key Laboratory of Low Dimensional Materials and Application Technology (Ministry of Education), Xiangtan University, Xiangtan, Hunan 411105, People's Republic of China*
[2]*Key Laboratory of Magnetic Materials and Devices, Ningbo Institute of Material Technology and Engineering, Chinese Academy of Sciences, Ningbo, Zhejiang 315201, People's Republic of China*
[3]*Laboratory of Magnetic Materials and Application Technology, Ningbo Institute of Material Technology and Engineering, Chinese Academy of Sciences, Ningbo 315201, People's Republic of China*
[4]*School of Materials Science and Engineering, Nanyang Technological University, Singapore 639798*

(Received 17 June 2014; accepted 1 September 2014; published online 11 September 2014)

The magneto-mechanical coupling effect of amorphous $Co_{40}Fe_{40}B_{20}$ (CoFeB) films (10-200 nm) on flexible polyethylene terephthalate substrates were investigated in detail. The normalized remanent magnetization (M_r/M_s) of CoFeB films changes significantly (up to 62%) under small tensile or compressive strain. Moreover, the thickness dependence of the magneto-mechanical coupling effect for the flexible CoFeB films was demonstrated. These results provide important information for the development of CoFeB-based magnetic tunnel junction used in flexible spintronic devices.
 [http://dx.doi.org/10.1063/1.4895628]

In spintronic devices such as magnetoresistive random access memories (MRAMs), information is stored by the direction of magnetization, which is controlled either by external magnetic fields or by spin polarized current.[1,2] Ferromagnetic materials with high spin polarization are preferred for spin-dependent transport in these devices. $Co_{40}Fe_{40}B_{20}$ possesses the highest spin polarization among the amorphous ferromagnetic Co-Fe-B alloys, and has shown very large tunneling magnetoresistance (TMR) in magnetic tunnel junctions (MTJ).[3–7] Spin polarized current flowing through an MTJ element will exert a spin torque to the magnetic moment in the free layer which can switch the magnetization if the current exceeds a threshold value.[8,9] The magnitude of threshold current depends on the free layer magnetization, film thickness, effective magnetic damping factor, and especially, the anisotropy field.[10–12]

Recently, flexible devices on plastic substrates have shown promise in applications including disposable electronics, smart cards, light-emitting diodes, signage, wearable electronics, and sensors.[13–16] For a magnetic material grown on flexible substrates, the substrate deformation will induce a tensile or compressive strain to the magnetic layer, which may change its anisotropy field.[17–20] Therefore, it is of vital importance to investigate the anisotropy field of CoFeB films under the influence of strain for the application of MTJ in flexible spintronic devices. So far, only few studies have reported the strain dependence of magnetic properties of CoFeB films.[21,22] In this work, we systematically study the strain-dependent magnetic anisotropy of amorphous CoFeB films grown on flexible polyethylene terephthalate (PET) substrates. It is observed that normalized remanent magnetization M_r/M_s of CoFeB films changes significantly (up to 62%) under a small tensile or compressive strain (less than 1%), and its magneto-mechanical coupling strength depends on the film thickness. These findings are of great importance for the development of flexible spintronic devices.

CoFeB thin films ranging from 10 to 200 nm were grown on PET (~200 μm) and Si substrates by dc magnetron sputtering at room temperature (RT). Before the deposition, the substrates were cleaned ultrasonically in ethanol, and then dried with argon gas. The base pressure of the sputtering chamber was below 7.5×10^{-5} Pa. During deposition, the argon flow was kept at 10 sccm and the pressure was set at 0.5 Pa. The deposition power and the distance between the target and the substrate were kept at 35 W and 50 mm, respectively. A thin Ta layer (~6 nm) was deposited to prevent the oxidation of CoFeB thin films.

Crystalline phases were analyzed using X-ray diffraction (XRD) with Cu-*K*a radiation ($\lambda = 0.1541$ nm). The film thickness was measured using a surface profilometer (KLA Tencor, Alpha-Step IQ) and cross-sectional field emission scanning electron microscopy (SEM, Hitachi, S-4800). The surface morphology of the films was characterized by atomic force microscopy (AFM) using Vecoo Dimension 3100 V. The angular dependence of hysteresis loops under different tensile and compressive strains generated via outward and inward bending of the samples were measured using vibrating sample magnetometer (VSM, Lakeshore 7410) at RT. The sample fixing processes on the molds are as following. First, the molds with different radii of curvature were designed to quantitative analysis of the effect of stress. The surface of molds is kept smooth and clean to make the consistency of stress. Second, the samples are fixed on the molds by double-sided tape. Finally, the samples were further fixed by nonmagnetic tape on the molds to keep the strain being fully transferred to the CoFeB films.

Figure 1(a) shows the XRD patterns of the as-deposited CoFeB films on PET with different thicknesses. It is clear

a)E-mail: wangbaomin@nimte.ac.cn.
b)E-mail: mhtang@xtu.edu.cn.
c)E-mail: runweili@nimte.ac.cn.

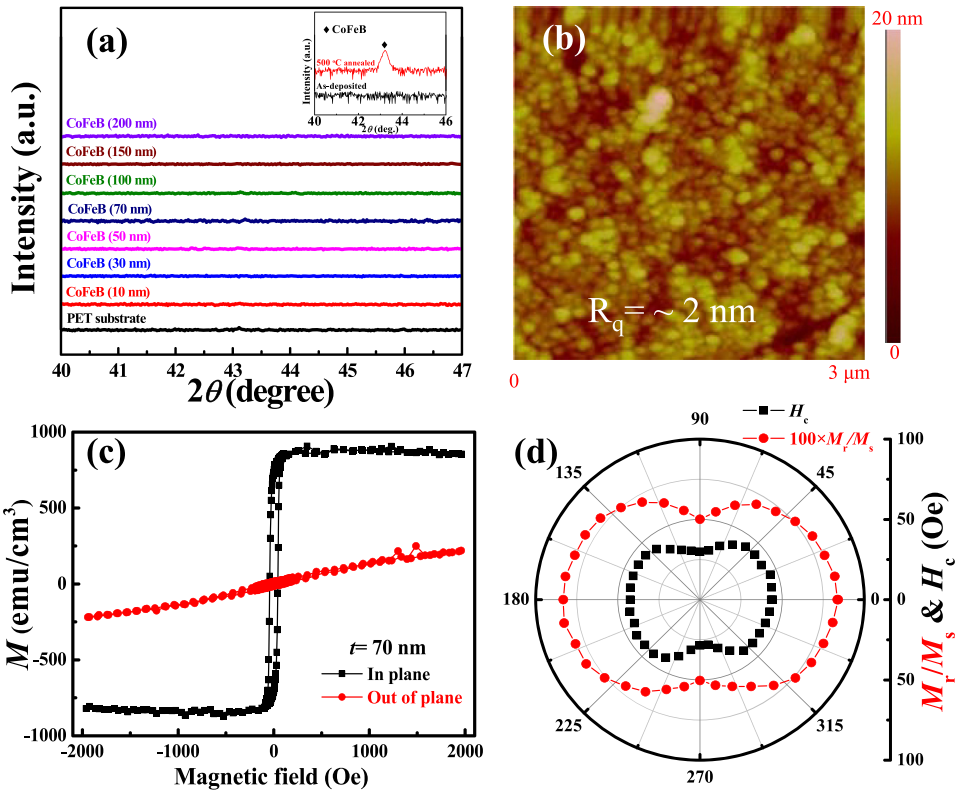

FIG. 1. (a) XRD patterns of the as-deposited CoFeB films on PET with different thicknesses. Inset: XRD patterns of the as-deposited and annealed CoFeB on Si. The characteristics for CoFeB (70 nm)/PET: (b) topography, (c) *M-H* hysteresis loops, (d) angular dependence of normalized M_r/M_s and H_c.

that the as-deposited CoFeB films are in the amorphous state. After being annealed at 500 °C, a distinct peak appears at $2\theta = 43.3°$ for CoFeB on Si substrate indicating the onset of crystallization [inset of Fig. 1(a)].[23,24] The amorphous CoFeB films with different thicknesses also have similar morphology characteristics. The topography of 70 nm CoFeB film shows that the thin film has a relative smooth surface with a small root mean square roughness (Rq ~ 2 nm) [Fig. 1(b)]. Figure 1(c) shows the magnetic hysteresis loops of 70 nm CoFeB film on PET substrate with magnetic field *H* parallel and perpendicular to the plane of film at RT. It is clear that the CoFeB film has an in-plane easy axis. In order to check the in-plane anisotropy, angular dependence of the magnetic hysteresis loop was measured at RT. Figure 1(d) shows the angular dependence of M_r/M_s and coercivity (H_c), which oscillate with 180° periodicity showing a uniaxial magnetic anisotropy. In contrast, the anisotropy of the reference samples grown on oxidized Si substrates is very weak (not shown). Therefore, we suggest that the uniaxial anisotropy of the CoFeB films on PET is due to the residual stress caused by the inevitable deformation of PET substrates during sample preparation. Due to both mechanical interlocking and chemical bonding between the CoFeB film and the PET substrate, the strain could be effectively transferred from the flexible substrates to the films.[18,25,26]

In order to study the strain-dependent magnetic anisotropy of amorphous CoFeB films systematically, we designed several molds with different radius to apply various tensile or compressive strains by pasting the flexible samples on the molds [Figs. 2(a) and 2(b)]. The strain on the flexible substrate using the molds can be fully transferred to the CoFeB films as the thickness of film (10–200 nm) is much smaller than that of substrate (200 μm). The applied strain/stress on amorphous CoFeB films is calculated as follows:[18,27]

$$\varepsilon_C = t/(2R - t), \tag{1}$$

$$\varepsilon_T = t/(2R + t), \tag{2}$$

$$\sigma = \varepsilon \times E_f/(1 - v^2), \tag{3}$$

where ε_C and ε_T are the tensile and compressive strains, *R* is the radius of the substrate, *t* is the thickness of the sample including the film thickness, E_f is the Young's modulus ($E_f = 160$ GPa for CoFeB), *v* is the Poisson ratio, and σ is the stress.[27,28] Equations (1) and (2) describe the compressive and tensile strains of the amorphous CoFeB films under inward and outward bending, respectively. Eq. (3) is the Hooke's law to describe the strain-stress relationship in two-dimensional thin films.[27] Consider the CoFeB film adhering to the substrate subjected to the tensile strain, the transverse compressive stress (σ_y) of the film is determined by the different transverse strains between film and substrate due to the difference of their Poisson ratio, which can be calculated by[29]

$$\sigma_y = E_f \times [-v_{substratte} \times \varepsilon_x^{substrate} + v_{CoFeB} \times \varepsilon_x^{CoFeB}]. \tag{4}$$

$v_{substrate}$ and v_{CoFeB} are Poisson ratios of PET (0.4) and CoFeB (0.3), respectively.[27,30] Assuming that the strain is fully transferred from PET to CoFeB, the strain of substrate is equal to that of film ($\varepsilon_x^{substrate} = \varepsilon_x^{CoFeB}$). The ratio between transverse and longitudinal stress (σ_x) in the CoFeB film is $|\frac{\sigma_y}{\sigma_x}| = |\frac{E_f \times [-v_{substratte} \times \varepsilon_x^{substrate} + v_{CoFeB} \times \varepsilon_x^{CoFeB}]}{\varepsilon_x^{CoFeB} \times E_f/(1-v_{CoFeB}^2)}| = 0.091$, which indicates that the stress in the CoFeB film is almost uniaxial and along the direction of longitudinal tensile strain. From the same analyses, we can also deduce the compressive stress applied in the present case is almost uniaxial.

Figure 2(c)–2(f) show the hysteresis loops of the 70 nm CoFeB film under various strains by slightly bending the

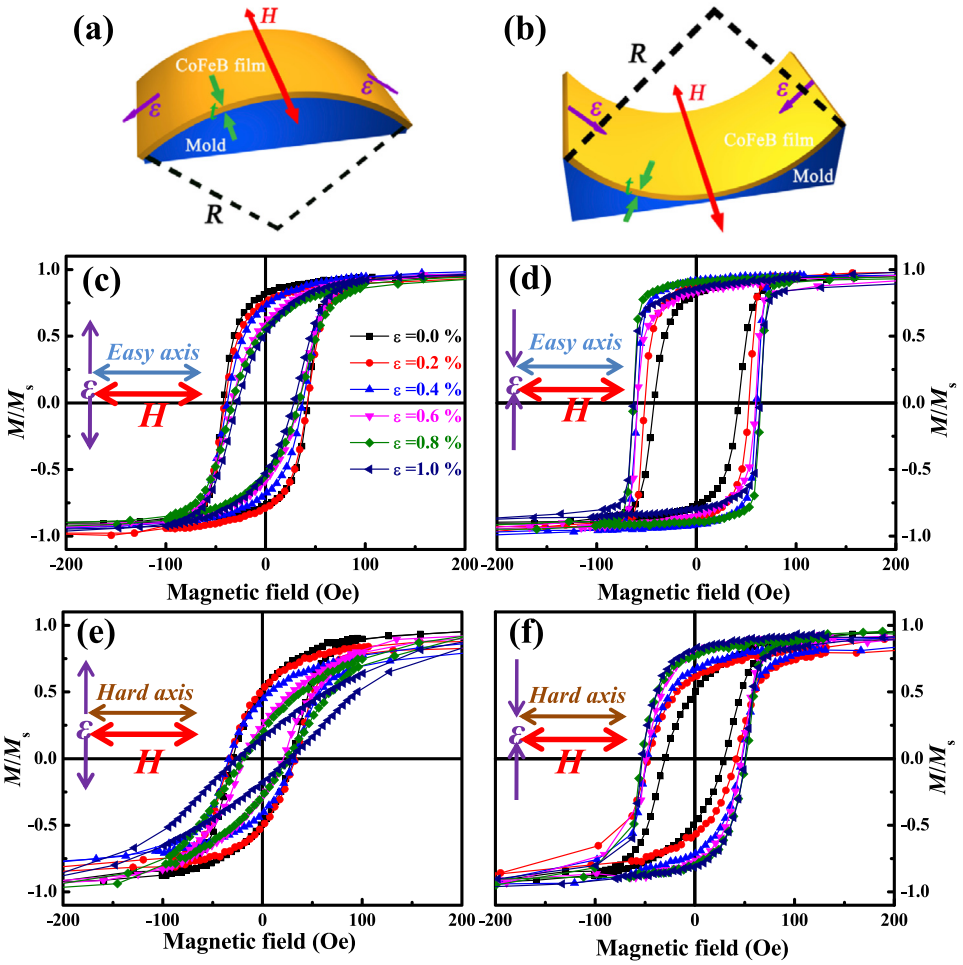

FIG. 2. The molds designed for applying strains: (a) tensile strain (b) compressive strain. Hysteresis loops of CoFeB (70 nm)/PET obtained under various external strains: (b) tensile strain, (c) compressive strain applied along the hard axis; (e) tensile strain, (f) compressive strain applied along the easy axis.

substrates along the easy or hard axes. The strains are applied from 0% to 1.0% with an increment of 0.2% by changing the radius of the molds. The surface morphology of the CoFeB film was examined using metallographic microscope and AFM under various strains (not shown). There is no crack in films for the strain applied less than 1.0%. However, if the strain increases to 2.0%, many cracks appear in the CoFeB film. Here, the maximum applied strain is 1.0% to assure that the tensile or compressive strains are fully transferred to CoFeB film. For all the magnetization measurements, the applied magnetic field is in-plane and perpendicular to the bending direction to make sure that the measured signals are from in-plane magnetic moments [Figs. 2(a) and 2(b)]. When the tensile (compressive) strain is applied, the M_r/M_s in the perpendicular direction decreases (increases) [Figure 2(c)–2(f)], which indicates that the anisotropy field of CoFeB can be changed by strain.

The strain dependence of the M_r/M_s and H_c for CoFeB on PET substrate is summarized in Fig. 3. Both of them can be tuned continuously under strains along easy or hard axis. For strain applied along hard (easy) axis, the M_r/M_s is changed from 0.88 (0.82) to 0.52 (0.16) between maximum tensile and compressive strains, which corresponds to ~29% (62%) variation. Moreover, the H_c also changes continuously under strains. Under our measurement configurations, the tensile strain leads to a decrease of M_r/M_s, while the compressive strain increases this value. The effect of a tensile strain applied along the easy axis is equivalent to that of a compressive strain along the hard axis, and vice versa. Our results suggest that easy (hard) axis of the CoFeB film can be tuned to hard (easy) axis under a tensile (compressive) strain applied along the hard (easy) axis or a compressive (tensile) strain along the easy (hard) axis. That is, the anisotropy fields of CoFeB films depend strongly on the applied strain through a magneto-mechanical coupling effect.

In addition, the CoFeB thickness (10–200 nm) dependence of magneto-mechanical coupling effect was also investigated in detail. Figure 4(a) and 4(b) show the hysteresis loops of 10 and 200 nm CoFeB films on PET at RT, respectively.

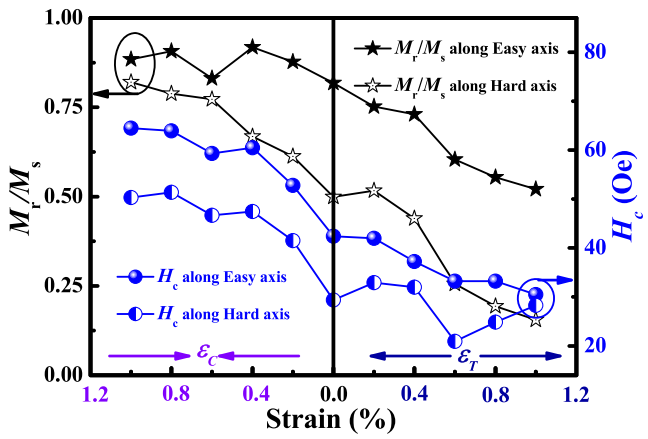

FIG. 3. The strains dependence of normalized M_r/M_s and H_c for strains applied along the easy and hard axes, respectively.

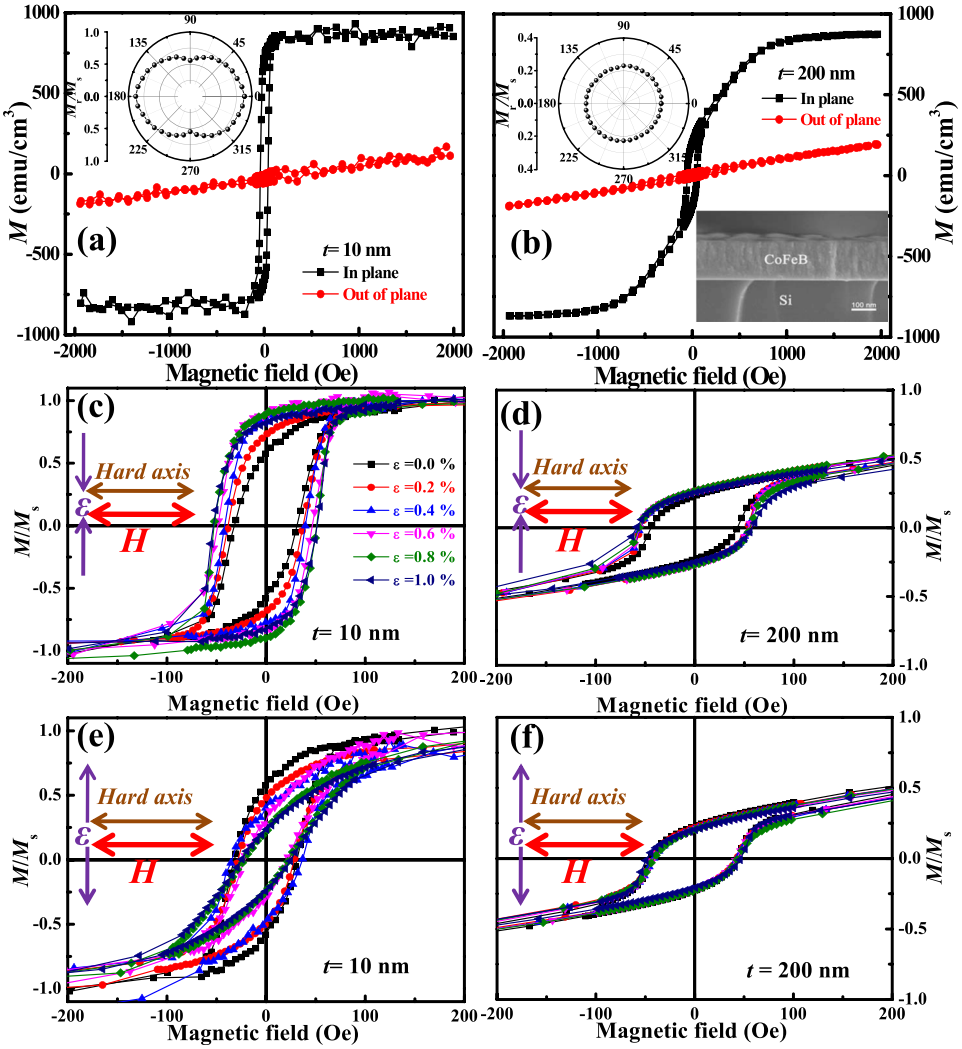

FIG. 4. Hysteresis loops for CoFeB/PET with different thickness: (a) 10 nm, (b) 200 nm. Inset: the angular dependence of normalized M_r/M_s and the cross-sectional SEM image of 200 nm CoFeB on Si. Hysteresis loops for CoFeB/PET with different thickness under various external strains along the hard axis: (c) compressive strain for 10 nm, (c) compressive strain for 200 nm, (e) tensile strain for 10 nm, (f) tensile strain for 200 nm.

The easy axes of both samples lie in the plane of film. Moreover, the residual stress-induced uniaxial anisotropy decreases with increasing thickness [inset of Figs 4(a) and 4(b)]. Figures 4(c)–4(f) show the strain-dependent magnetic anisotropy of 10 and 200 nm CoFeB. Similar mechanically tunable magnetic properties were observed in the 10 nm CoFeB film [Figs. 4(c) and 4(e)]. However, the magneto-mechanical coupling became very weak for the 200 nm sample. The M_r/M_s dependence of strain in amorphous CoFeB on PET with different thickness is shown in Fig. 5. The results show a critical thickness $\sim$ 150 nm, below which anisotropy field of CoFeB film is strongly dependent on the applied strain. The possible reasons could be as follows: On the one hand, the strain transmission from substrate to thicker CoFeB film will decrease since the Young's modulus difference between CoFeB and PET substrate, which may contributes to its insensitivity for stress;[31] On the other hand, the formation of columnar crystals was observed by cross-section SEM image [inset of Fig. 4(b)]. The column of columnar crystals is insensitive to stress under various mechanical strains, inward or outward bending of the films, because of the reduction of the pressed area of column by comparison with the granular films.[32,33] Furthermore, the grain boundaries of columnar crystals may migrate under the drive of stress without

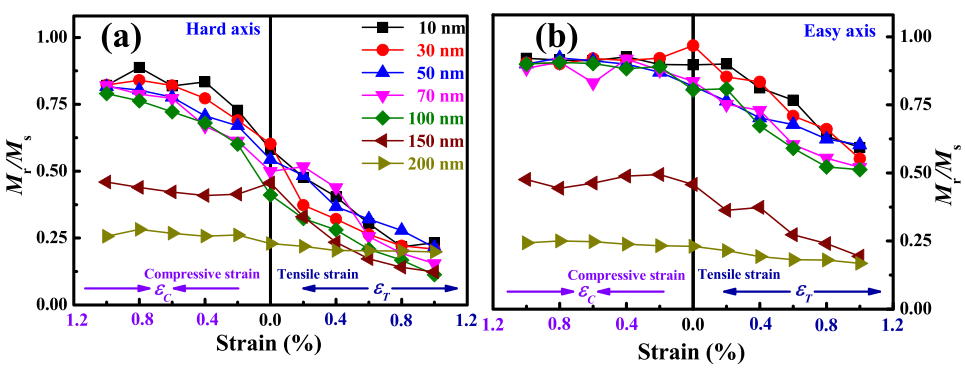

FIG. 5. The strain dependence of M_r/M_s for CoFeB on PET with different thickness.

changes of the distribution of magnetic moment, which could lead to the reduction of the effect of stress on magnetic properties.[33–36]

In summary, we fabricated amorphous CoFeB films on flexible PET substrates by dc-sputtering. The magneto-mechanical coupling effect is studied under various compressive or tensile strains generated by the inward or outward bending of the films. The M_r/M_s ratio and coercivities are tuned by strains applied along the easy or hard axis of the CoFeB films, and the results indicate that the easy axis can be changed to hard axis and vice versa. Furthermore, thickness dependent study reveals a critical thickness of 150 nm, above which the strain effect is much weaker. Our study suggests that we can tune the anisotropy field of CoFeB film by strain, thus controlling the threshold current in magnetic tunnel junctions such as CoFeB-MgO-CoFeB. The findings are of importance for realizing better performance in MRAMs and for development of flexible spintronics.

This work was financially supported by the National Natural Science Foundation of China (Nos. 51301191, 11304326, and 61274107), the Ningbo Science and Technology Innovation Team (Nos. 2011B82004).

[1]L. Berger, Phys. Rev. B **54**, 9353 (1996).
[2]M. Endo, S. Kanai, S. Ikeda, F. Matsukura, and H. Ohno, Appl. Phys. Lett. **96**, 212503 (2010).
[3]Y. M. Lee, J. Hayakawa, S. Ikeda, F. Matsukura, and H. Ohno, Appl. Phys. Lett. **90**, 212507 (2007).
[4]T. Kubota, T. Daibou, M. Oogane, Y. Ando, and T. Miyazaki, Jpn. J. Appl. Phys., Part 2 **46**, L250 (2007).
[5]S. S. P. Parkin, C. Kaiser, A. Panchula, P. M. Rice, B. Hughes, M. Samant, and S. H. Yang, Nat. Mater. **3**, 862 (2004).
[6]D. D. Djayaprawira, K. Tsunekawa, M. Nagai, H. Maehara, S. Yamagata, N. Watanabe, S. Yuasa, Y. Suzuki, and K. Ando, Appl. Phys. Lett. **86**, 092502 (2005).
[7]S. Ikeda, K. Miura, H. Yamamoto, K. Mizunuma, H. D. Gan, M. Endo, S. Kanai, J. Hayakawa, F. Matsukura, and H. Ohno, Nat. Mater. **9**, 721 (2010).
[8]A. Brataas, A. D. Kent, and H. Ohno, Nat. Mater. **11**, 372 (2012).
[9]W. G. Wang, S. Hageman, M. Li, S. Huang, X. Kou, X. Fan, J. Q. Xiao, and C. L. Chien, Appl. Phys. Lett. **99**, 102502 (2011).
[10]Y. F. Chen, Y. F. Mei, R. Kaltofen, J. I. Monch, J. Schumann, J. Freudenberger, H. J. Klauß, and O. G. Schmidt, Adv. Mater. **20**, 3224 (2008).
[11]J. Z. Sun, Phys. Rev. B **62**, 570 (2000).
[12]S. H. Chen, M. H. Tang, Z. Z. Zhang, B. Ma, S. T. Lou, and Q. Y. Jin, Appl. Phys. Lett. **103**, 032402 (2013).
[13]H. T. Yi, M. M. Payne, J. E. Anthony, and V. Podzorov, Nat. Commun. **3**, 1259 (2012).
[14]X. W. Wang, Y. Gu, Z. P. Xiong, Z. Cui, and T. Zhang, Adv. Mater. **26**, 1336 (2014).
[15]M. L. Hammock, A. Chortos, B. C. K. Tee, J. B. H. Tok, and Z. Bao, Adv. Mater. **25**, 5997 (2013).
[16]S. R. Forrest, Nature **428**, 911 (2004).
[17]T. Uhrmanna, L. Bara, T. Dimopoulosa, N. Wiesea, M. Ruhriga, and A. Lechnerb, J. Magn. Magn. Mater. **307**, 209 (2006).
[18]G. H. Dai, Q. F. Zhan, Y. W. Liu, H. L. Yang, X. S. Zhang, B. Chen, and R. W. Li, Appl. Phys. Lett. **100**, 122407 (2012).
[19]S. F. Zhao, J. G. Wan, M. L. Yao, J. M. Liu, F. Q. Song, and G. H. Wang, Appl. Phys. Lett. **97**, 212902 (2010).
[20]G. H. Dai, Q. F. Zhan, H. L. Yang, Y. W. Liu, X. S. Zhang, Z. H. Zuo, B. Chen, and R. W. Li, J. Appl. Phys. **114**, 173913 (2013).
[21]A. T. Hindmarch, A. W. Rushforth, R. P. Campion, C. H. Marrows, and B. L. Gallagher, Phys. Rev. B **83**, 212404 (2011).
[22]Y. T. Chen, S. U. Jen, Y. D. Yao, J. M. Wu, and A. C. Sun, Appl. Phys. Lett. **88**, 222509 (2006).
[23]H. Fulara, S. Chaudhary, S. C. Kashyap, and D. K. Pandya, J. Appl. Phys. **110**, 093916 (2011).
[24]P. V. Paluskar, J. T. Kohlhepp, H. J. M. Swagten, and B. Koopmans, J. Appl. Phys. **99**, 08E503 (2006).
[25]S. S. P. Parkin, Appl. Phys. Lett. **69**, 3092 (1996).
[26]X. S. Zhang, Q. F. Zhan, G. H. Dai, Y. W. Liu, Z. H. Zuo, H. L. Yang, B. Chen, and R. W. Li, Appl. Phys. Lett. **102**, 022412 (2013).
[27]D. Wang, C. Nordman, Z. Qian, J. M. Daughton, and J. Myers, J. Appl. Phys. **97**, 10C906 (2005).
[28]K. Y. Wang, K. W. Edmonds, R. P. Campion, L. X. Zhao, C. T. Foxon, and B. L. Gallagher, Phys. Rev. B **72**, 085201 (2005).
[29]J. Andersons, S. Tarasovs, and Y. Leterrier, Thin Solid Films **517**, 2007 (2009).
[30]Y. Leterrier, A. Mottet, N. Bouquet, D. Gilliéron, P. Dumont, A. Pinyol, L. Lalande, J. H. Waller, and J.-A. E. Månson, Thin Solid Films **519**, 1729 (2010).
[31]Y. Zhang, J. Appl. Mech. **75**, 011008 (2008).
[32]O. Perevertov and R. Schäfer, J. Phys. D: Appl. Phys. **45**, 135001 (2012).
[33]X. Tang, X. Zhang, R. Tao, and Y. Rong, J. Appl. Phys. **87**, 2634 (2000).
[34]T.-S. Ke, Phys. Rev. **72**, 41 (1947).
[35]S. Bliigel, Phys. Rev. B **51**, 2025 (1995).
[36]T. J. Rupert, D. S. Gianola, Y. Gan, and K. J. Hemker, Science **326**, 1686 (2009).